Article:
Liu, K orcid.org/0000-0001-8985-7294, De Boar, EL, Yao, Y et al. (3 more authors) (2016) Heterogeneous Distribution of Entanglements in a Nonequilibrium Polymer Melt of UHMWPE: Influence on Crystallization without and with Graphene Oxide. Macromolecules, 49. pp. 7497-7509. ISSN 0024-9297

https://doi.org/10.1021/acs.macromol.6b01173

Heterogeneous distribution of entanglements in a non-equilibrium polymer melt of UHMWPE; influence on crystallization with, and without, graphene oxide

Kangsheng Liu[†+], Ele de Boer[†], Yefeng Yao[§], Dario Romano[†,‡], Sara Ronca[†*], Sanjay Rastogi[†,‡*]

† Department of Materials, Loughborough University, Loughborough, LE11 3TU, UK

‡ Department of Biobased Materials, Faculty of Humanities and Sciences, Maastricht University, P.O. Box 616, 6200MD, Maastricht, The Netherlands

§ Shanghai Key Laboratory of Magnetic Resonance, East China Normal University, North Zhongshan Road 3663, 200062 Shanghai, PR China

+ Textile Materials Technology Group, School of Design, University of Leeds, Leeds, LS2 9JT, UK

*Corresponding Authors: sanjay.rastogi@maastrichtuniversity.nl; s.ronca@lboro.ac.uk

Abstract

Recently, the influence of reduced graphene oxide nanoplatelets (rGON) on the rheological response of polymers has been a subject of interest. In the case of disentangled UHMWPE, it has been shown that the chain-filler interaction in the UHMWPE/rGON composite results into an everlasting non-equilibrium melt state having heterogeneous distribution in entanglement density. In this study, a thermal analysis protocol is used to follow the influence of the non-equilibrium polymer melt on the crystallization kinetics of disentangled UHMWPE with, and without, rGON. The analysis is carried out by means of differential scanning calorimetry (DSC) and the results are supported by rheology. When the disentangled UHMWPE sample, without the filler rGON, is left to crystallize under isothermal condition after melting, two endothermic peaks are observed: the high temperature peak (close to the equilibrium melting point, 141.5 °C) is related to the melting of crystals obtained on crystallization from the disentangled domains of the heterogeneous (non-equilibrium) polymer melt, whereas the low melting temperature peak is related to the melting of crystals formed from entangled domains of the melt. On increasing the annealing time in melt (160 °C), the enthalpy of the lower melting temperature peak increases at the expense of the high melting temperature peak, confirming a transformation of the non-equilibrium polymer melt to a fully entangled equilibrium melt state. However, independent of the equilibrium or non-equilibrium melt state, the recurrence of the high melting temperature peak is observed when the samples synthesized using the single-site catalytic system are left to isothermal crystallization at a specific temperature. The recurrence of the high melting temperature, close to the equilibrium melting point of the polymer, questions the differences in entanglements formed before and after polymerization in these high molar masses. The differences in the topological constraints are likely to influence the difference in melting temperatures of the isothermally crystallized samples. In the presence of rGON, the melting response of disentangled UHMWPE crystallized from its heterogeneous melt state changes; at a specific filler concentration, it is observed that the high endothermic peak remains independent of the annealing time in melt. This observation strengthens the concept that in the presence of the filler, chain dynamics is arrested to an extent that the non-equilibrium melt state having lower entanglement density is retained, facilitating the formation of crystals having high melting temperature.

1.0 Introduction

The topology of methylene segments in the non-crystalline region of the semi-crystalline polymer Ultrahigh Molecular Weight Polyethylene (UHMWPE), has a profound influence on the mechanical deformation either uniaxially or biaxially [1]. The topology can be tailored by controlling the crystallization kinetics either by dissolution and crystallization or controlled polymerization [2,3,4,5]. The influence of molar mass on the topology of non-crystalline phase has been a subject of interest where the nature of the mobile phase is probed by solid state NMR [6, 7]. Yao et al. investigated the influence of polymerization conditions on the non-crystalline region of the semi-crystalline region [7]. To recall, the authors demonstrated that the non-crystalline region in the polymer synthesized using Ziegler-Natta differed from the polymer synthesized using a single-site catalytic system [7].

The absence of structural order in the non-crystalline region of semi-crystalline polymers imposes challenges to an extent that the issue of adjacent or non-adjacent re-entry remains unsolved even today, despite the discovery of chain folded crystals in 1957 [2,8,9]. Recently, in UHMWPE, it has been shown that the melting temperature of the as-synthesized polymer (nascent) approaches the equilibrium melting temperature because of the restricted mobility of the methylene segments in the non-crystalline region [10]. Differentiation between the non-crystalline regions of the polymer synthesized using Ziegler-Natta (Z-N) and single site catalytic systems can be made by following kinetics in the melting of the crystals [7,10]. To recall, when the nascent sample is left to anneal at the onset of the melting temperature of the endothermic peak, having peak melting temperature close to 141.5 °C, crystals tend to melt via consecutive detachment of chains from the crystal surface followed by reeling-in of the chain stems into melt [10]. The rate at which the consecutive detachment occurs is suggested to be dependent on the polymerization conditions i.e. topological constraints and entanglements present in the non-crystalline region. Combining the NMR observations on segmental mobility in the non-crystalline region and melting kinetics of crystals, the high temperature melting peak of the nascent crystals is shown to be related with the restriction imposed by the non-crystalline region. Combining the mechanical deformation characteristics of the nascent UHMWPE crystals in solid-state with the melting kinetics, it is well understood that the topological constraints in the non-crystalline region can be tailored by controlling crystallization kinetics during polymerization.

Upon melting, the nascent crystals, having reduced number of entanglements, results into a non-equilibrium polymer melt where the initial low elastic shear modulus increases with time till the melt reaches the equilibrium state. Time required in build-up of the shear elastic modulus is shown to be dependent on the molar mass following the power law $t_{build\text{-}up} \sim M^{2.6}$ [11]. The non-equilibrium polymer melt is suggested to have heterogeneous distribution of entanglements, with domains having low and high density of entanglements [5]. This heterogeneity in the distribution of entanglements will have implications on crystallization kinetics. For an example, chain segments in the low density entanglement domains are likely to have lower nucleation barrier for crystallization compared to the segments in the high density entanglement domains [12,13,14,15].

Here we investigate the influence of heterogeneous melt having inhomogeneous distribution of entanglement density on crystallization kinetics. Nascent disentangled UHMWPE, synthesized using a single-site catalytic system under controlled conditions [1,5], provides a unique opportunity to investigate the influence of heterogeneity in entanglements on crystallization. For the purpose, a specific thermal protocol is applied where the residence time of the polymer in its non-equilibrium melt state is varied. Thus by increasing the residence time in the melt, with increasing elastic shear modulus, the overall entanglement density of the polymer melt is increased. Crystallization kinetics of the heterogeneous melt has been pursued by annealing the sample below the equilibrium melting temperature. At a critical crystallization temperature (128 °C), where the nucleation rate dependence on supercooling is suppressed, the existence of heterogeneous entanglement distribution is unveiled in the form of two endothermic peaks on re-heating the annealed sample to melt. The high temperature endothermic peak (141.5 °C) is found to be close to the equilibrium melting temperature, whereas the low temperature endothermic (135 °C) peak is related to the component that did not crystallize at isothermal condition. These observations will be related to the elastic shear modulus build-up of the polymer, reflecting the homogenization of the heterogeneous distribution of entanglements in melt state. The conclusions drawn are strengthened by investigating composites of polyethylene with rGON. What follows are the experimental findings on the nascent disentangled polymer, where a commercial UHMWPE, having entangled nascent crystals and synthesized using a Z-N catalyst, is used as a comparative example.

2.0 Experimental

2.1 Materials

Toluene (99.8%, anhydrous) and methyaluminoxane solution (MAO, 10 wt % solution in toluene) were purchased from Sigma-Aldrich; ethylene (grade 3.0) was purchased from BOC, and bis[N-(3-tertbutylsalicylidene)pentafluoroanilinato]titanium (IV) dichloride (FI) catalyst was purchased from MCat. Materials for the synthesis of graphene oxide were purchased from Sigma-Aldrich: fine graphite powder (diameter of c.a. 25 μm), 98 wt % concentrated sulphuric acid, distilled water, potassium permanganate, and 30 wt % hydrogen peroxide. Commercial UHMWPE powder was purchased from Sigma-Aldrich (Catalogue No. 429015). Antioxidant Irganox 1010 was purchased from Ciba. All reagents were used as received.

2.2 Synthesis of disentangled UHMWPE

The disentangled UHMWPE samples were synthesized using the same polymerization method described in ref [17]. Polymerization with different reaction times, 10 min and 30 min, were carried out for the study.

The obtained polymers were then filtered, and further washed with copious amount of methanol/acetone. To achieve a good dispersion of antioxidant, 0.7-1.0 wt % antioxidant was then added to the polymers suspended in acetone and stirred under a fume hood. After all the acetone had evaporated, the polymer was further dried in a vacuum oven at 40 °C for 720 min.

2.3 Synthesis of GON and preparation of composites

The GON was synthesized in accordance with a modified Hummers method [16] with further modifications as described in ref [17]. To recall, after the oxidation reaction was finished, the resultant material was repeatedly vacuum-filtered and washed 3 times with 5 wt % HCl and few times with distilled water. The extracted suspension having GON became darker with the increasing number of washing steps, suggesting progressive extraction of GON from the bottom layer to the upper suspension. The average number of water washing steps applied was approximately ten, until the pH of the suspension changed from ~2 to ~7. The previously

collected dark-liquid portions were combined and dried in a petri dish at 50 ºC for 2 days. Films of GON were obtained by peeling them off from the petri dish.

The composites of disentangled UHMWPE (synthesized for 30 min) and GON were made using a two-step preparation method, as described in ref [17]: composites having GON content of 0.1 wt % and 0.8 wt % were prepared using the same method. GON reduces to rGON when the composites are thermally treated at 160 °C [18].

2.4 Determination of molar mass and molar mass distribution

Weight-average molecular weight (M_w) and polydispersity index (PDI) of the synthesized disentangled UHMWPEs and commercial UHMWPE were estimated by melt rheology using the Advanced Rheometrics Expansion System (ARES) of TA instruments; the results are shown in Table 1, and the method for calculation has been described elsewhere [4,19,20].

Table 1 Molecular characteristics of the UHMWPE samples; C-PE refers to commercial UHMWPE and Dis-PE represents disentangled UHMWPE.

Samples	**M_w ($\times 10^6$ g/mol)**	**PDI**	**G_N^0@10 rad/s (MPa)***
C-PE	4.5	31.1	2.0
0.8 wt % C-PE/rGON	4.5	31.1	2.0
Dis-PE-1 (30 min-reaction)	4.8	3.1	2.0
0.1 wt % Dis-PE-1/rGON	4.8	3.1	1.8
0.8 wt % Dis-PE-1/rGON	4.8	3.1	0.8
Dis-PE-2 (10 min-reaction)	2.0	2.3	2.0

*G_N^0 is determined from dynamic frequency sweep after the samples have reached the plateau value in elastic shear modulus build-up. For details on the rheological studies, please see refs [19,21].

2.5 Thermal Analysis

A Q-2000 MDSC from TA instruments was used to follow the crystallization kinetics and subsequent melt enthalpies. High precision T_{Zero} pans with lids were used for the experiments. To minimize the thermal lag caused by the samples, the weight is kept within 1.5±0.1 mg for each sample. During the measurement, nitrogen was continuously purged at 50 mL/min. Temperature and enthalpy calibrations were conducted using certified Indium at the heating

rate applied for the samples. A thermal protocol has been devised to obtain samples having different entanglement densities and to follow the crystallization kinetics and enthalpies. The protocol is given in Scheme 1.

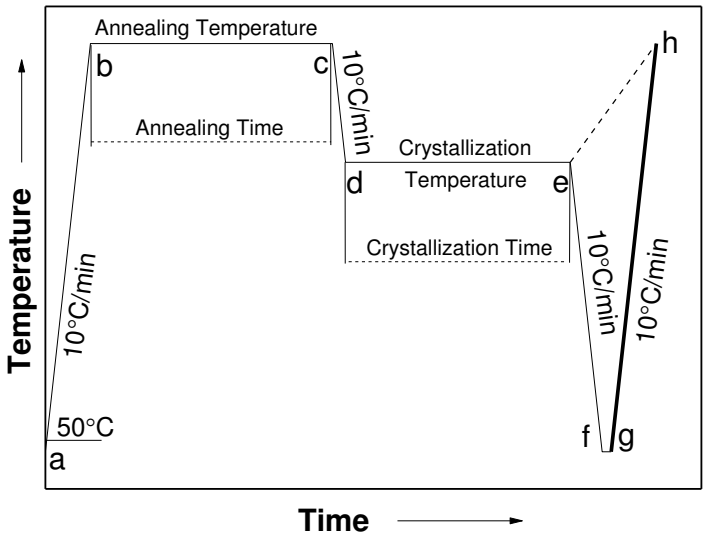

Scheme 1 Thermal analysis protocol; in b-c different annealing times are chosen to vary entanglement density in melt; in d-e isothermal crystallization at different crystallization temperatures and crystallization time is performed.

(a-b) Heating from 50 °C to an annealing temperature which is higher than PE's equilibrium temperature (141.5 °C) at 10 °C/min, for instance 160, 170, 180 and 190 °C;

(b-c) Annealing for a fixed time (5, 30, 60, 180, 360, 720 and 1440 min, respectively);

(c-d) Cooling to an isothermal crystallization temperature, for example 120, 122, 124, 126, 128 °C, at 10 °C/min;

(d-e) Isothermal crystallization at the isothermal crystallization temperature for a fixed time, for instance, 60, 180, 300 min;

(e-f) Cooling to 50 °C at 10 °C/min;

(g-h) Second heating from 50 ºC to 160 °C at 10 °C/min.

The DSC plots shown in the results and discussion section were obtained during the ramp **g-h**.

2.6 Rheology Measurements

The nascent powders of disentangled UHMWPE were compressed into a plate having diameter of 50 mm and thickness of c.a. 0.7 mm at a fixed temperature of 125 °C, combined with pressures of 510 bars for 5 min, 1020 bars for 10 min and 2040 bars for 5 min. For sintering, the C-PE powders were compressed at 160 ºC under the same pressures and times. Disks with 12 mm diameter were cut from the compressed plate using a hollow punch for the rheology measurements. The rheological measurements were performed using the protocol described in ref 17.

3.0 Results and Discussion

3.1 Crystallization in heterogeneous polymer melt

Disentangled UHMWPE used in this study has unique features, for instance, significant low initial entanglement density, high number-average molecular weight (M_n), and relatively low molar mass distribution. Extensive studies on chemistry and physics of the UHMWPE have been carried out [4,10,22,23]. To recall, due to the high solubility of the catalyst in the polymerization medium, toluene for instance, a uniform distribution of active sites across the medium becomes feasible. To lower the possibility of entanglement formation during the synthesis, the concentration of the active sites is kept low. In addition, the catalyst activity is maintained high even at relatively low polymerization temperature (10 °C for instance). It is important to notice that at these low temperatures the crystallization rate is sufficiently high to promote crystallization within the first few seconds of ethylene uptake. As a result, the synthesized polymer has a very low entanglement density as well as high M_n and low molar mass distribution. However, once the semi-crystalline polymer is molten the ‘disentangled’ polymer chains in the non-crystalline phase tend to entangle leading to heterogeneous distribution of entanglement density in melt. The change in entanglement density with time could be followed by rheology [5,10]. The observations are that the shear elastic modulus with time increases; ultimately transforming the non-equilibrium melt to the equilibrium state and leading to the homogeneous distribution of entanglements. Figure 1a shows the elastic shear modulus build-up of a disentangled sample, Dis-PE-1, and an entangled UHMWPE sample, C-PE. The latter is used as a reference sample synthesized using a Z-N catalyst where the entanglements are built-in during synthesis. Important to note is that while the

disentangled UHMWPE synthesized using a single-site catalyst shows continuous increase in the storage modulus, the entangled C-PE hardly shows any increase in the storage modulus. The rheological experiments for the two samples have been performed under the same conditions.

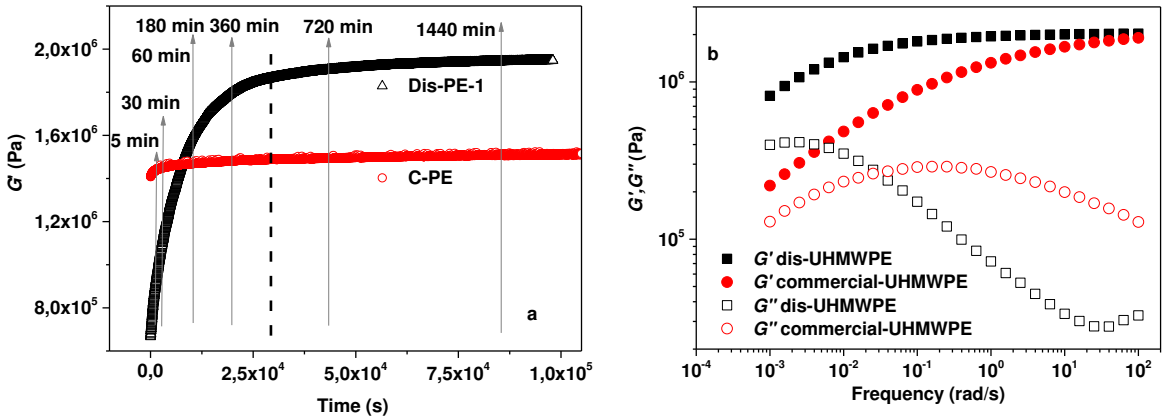

Figure 1 a) Elastic shear modulus build-up of disentangled (open triangle) and entangled UHMWPE (open cycle); the measurements were carried out at 160 °C, at a constant frequency of 10 rad/s and constant strain of 0.5 % (well within the linear viscoelastic regime); the arrows show a selection of annealing time at 160 °C that have been used in the DSC measurements, b-c in Scheme 1, in order to create samples with different entanglement density; **b)** Frequency sweep of the polymers after reaching plateau are shown in **a)**.

The near absence of elastic shear modulus build-up in the entangled UHMWPE, compared to the disentangled UHMWPE, suggests that the sample synthesized using Ziegler-Natta catalyst approaches equilibrium melt state much faster than the sample synthesized using the single-site FI catalytic system, Figure 1a. The continuous shear modulus build-up of disentangled sample indicates that before reaching the thermodynamic equilibrium state, the polymer melt stays in a non-equilibrium state, where M_e (the molar mass between entanglements) is considerably higher than the equilibrium value. To recall, M_e can be related to the elastic shear modulus at rubbery plateau as described in equation (1) [21,24].

$$G_N^o = \frac{g_N \rho RT}{<M_e>} \qquad \text{(Equation 1)}$$

where G_N^o is the plateau modulus at thermodynamic equilibrium state; $<M_e>$ is the average molecular weight between adjacent entanglements and it is inversely proportional to the entanglement density; g_N is a numerical factor (could be 4/5 or 1 depending on convention); ρ is the density of the material at the absolute temperature T, where R is the gas constant.

The heterogeneity in the entanglement density of the disentangled samples is created by keeping the polymer melt for different annealing times, for example at 160 °C. The annealing times are chosen by referring back to the modulus build-up, as shown in Figure 1a. After annealing, the samples were cooled to 128 °C where they were subjected to isothermal crystallization for 180 min. Prior to the second heating, g-h, the samples were cooled to 50 °C at 10 °C/min, e-f, Scheme 1. The DSC curves obtained during the heating ramp, g-h, are plotted in Figure 2a, and for comparison, the entangled commercial C-PE was subjected to the same thermal protocol and the results are plotted in Figure 2b.

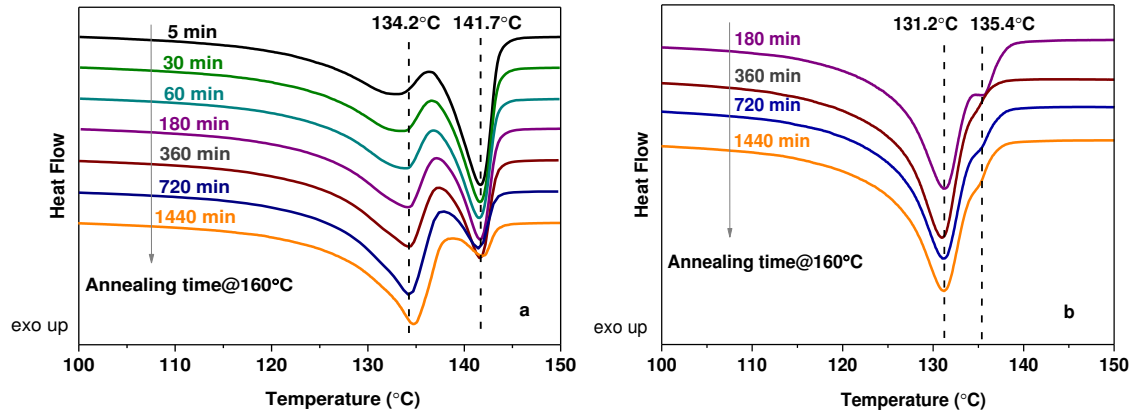

Figure 2 DSC plots, obtained from cycle g-h of Scheme 1 where the samples were annealed at 160 ºC for different times, the isothermal crystallization after annealing was done at 128 C for 180 min **a)** Dis-PE-1 samples annealed at 160 ºC for different times selected according to Figure 1a; **b)** refers to C-PE samples. For the enthalpy values please refer to Tables S1 and S2 in the supplementary section.

The disentangled UHMWPE samples show two separate melting peaks after annealing and isothermal crystallization, Figure 2a, with a lower temperature melting peak at 134.5 °C and a higher temperature melting peak close to 141.5 °C, indicating crystallization from entangled and disentangled domains of the heterogeneous polymer melt, respectively. The melting peak at 141.5 °C is close to the equilibrium melting temperature, which following the Gibbs-Thomson equation refers to extended chain crystals or the nascent crystals having restricted mobility in the non-crystalline region. The area-ratio between the low and the high melting temperature peaks changes with the annealing time of the melt at 160 °C. Considering the elastic shear modulus build-up with the annealing time at 160 °C and the corresponding transformation of the heterogeneous melt into homogeneous, the increase in the heat of fusion of the low melting temperature peak is attributed to the entangled state of the melt that causes increase in the nucleation barrier during isothermal crystallization [12,13,14,15].

The absence of the prominent double-peak and the inversion process in the comparative commercial sample, Figure 2b, further strengthens the hypothesis that in the disentangled UHMWPE, the transformation of the heterogeneous distribution of entanglement density into homogeneous has an influence on the increase in the low temperature peak.

To have further insight into the origin of the double-peak in the disentangled UHMWPE; the samples were left to crystallize at different temperatures, d-e in the Scheme 1 for isothermal crystallization time of 180 min after being annealed in melt, b-c, for 60 min. The observations are that the endothermic peak observed on heating from g-h shows gradual shift from 135 °C to 141.5 °C with increasing crystallization temperature from 120 °C to 126 °C, Figure 3a. The shift to the higher temperature, with increasing the crystallization temperature, is in good agreement with the earlier findings and can be explained by the increase in crystal thickness and/or crystal perfection [25,26]. However, the appearance of high endothermic peak at 141.5 °C (independent of the annealing time and annealing temperature in melt and will be discussed later e.g. Figure 6) is unique and appears to be a characteristic of disentangled UHMWPE that requires further consideration. Above the annealing temperature of 126 °C, Figure 3a, the appearance of a low temperature endothermic peak together with the high temperature endothermic peak, on heating the sample along g-h, is observed. The enthalpy of the low temperature endothermic peak increases with the crystallization temperature. The presence of the low temperature peak and the associated heat of fusion can be explained by the higher nucleation barrier at lower supercoolings. Thus the origin of the low temperature endothermic peak is related to the melt crystallized component of the sample on cooling from e-f, whereas the high temperature endothermic peak is related to the crystalline component obtained during isothermal crystallization. The comparative example of commercial sample also shows the presence of two peaks on crystallization at lower supercoolings, in Figure 3b. However, unlike the disentangled sample, the high temperature endothermic peak is found to be around 134 °C which is not surprising and is in agreement with earlier findings on linear polyethylenes [27].

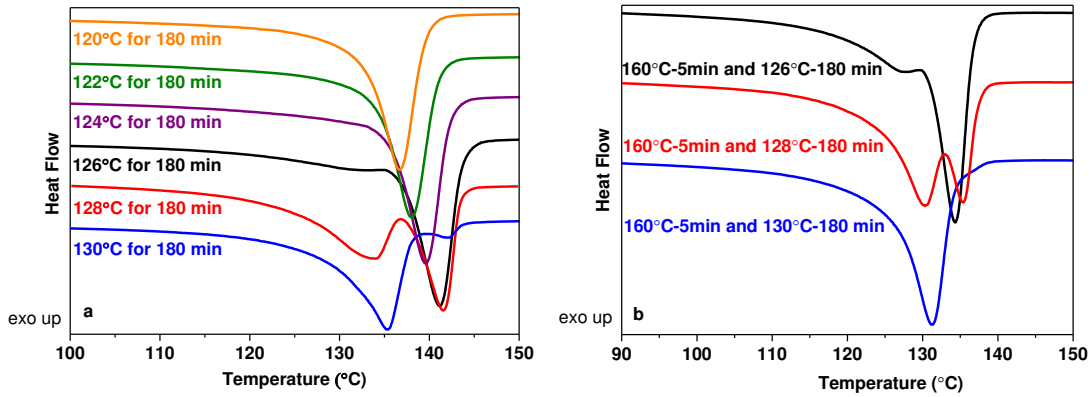

Figure 3 DSC plots, obtained from ramp g-h of Scheme 1, of **a)** Dis-PE-1 samples annealed at 160 ºC for 60 min and isothermally crystallized for 180 min at different temperatures (120, 122, 124, 126, 128, 130 ºC respectively), and **b)** C-PE samples annealed at 160 ºC for 5 mins and isothermally crystallized for 180 min at different temperatures (126, 128, 130 ºC respectively). For enthalpy values of Figure 3a please refer to Table S3 in the supplementary section.

To have further insight on the origin of the double peak in disentangled UHMWPE, the sample of Dis-PE-2 was left to crystallize at 128 °C for different times, ranging from 60 min to 300 min. With increasing isothermal crystallization time, the high temperature endothermic peak increases in enthalpy at the expense of the low temperature endothermic peak, Figure 4. This result further confirms that the enthalpy related to the high temperature endothermic peak is dependent on the supercooling that influences the nucleation density of the polymer.

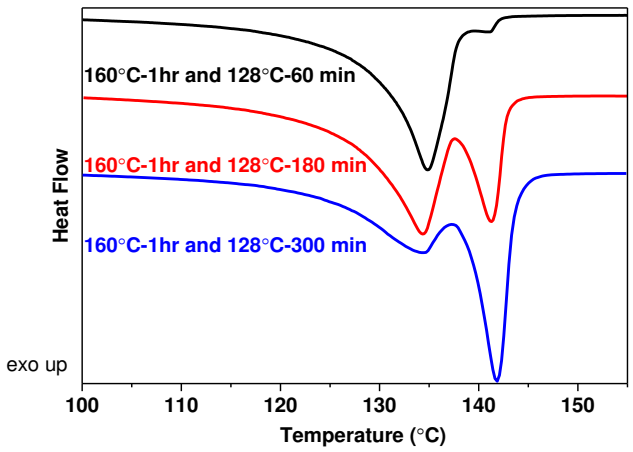

Figure 4 DSC plots, obtained from cycle g-h of Scheme 1, of Dis-PE-2 samples annealed at 160 ºC for a fixed time and isothermally crystallized at 128 °C for different times (60, 180, 300 min respectively). For enthalpy values please refer to Table S4 in the supplementary section.

To rule out the possibility on formation of crystals, contributing to low temperature endothermic peak during isothermal crystallization, a sample was annealed at 160 ºC for 60

min; isothermally crystallized at 128 ºC for 180 min and then heated directly to 160 ºC (i.e. creating new pathway e-h in Scheme 1). As expected, only the high temperature endothermic peak is observed, Figure 5.

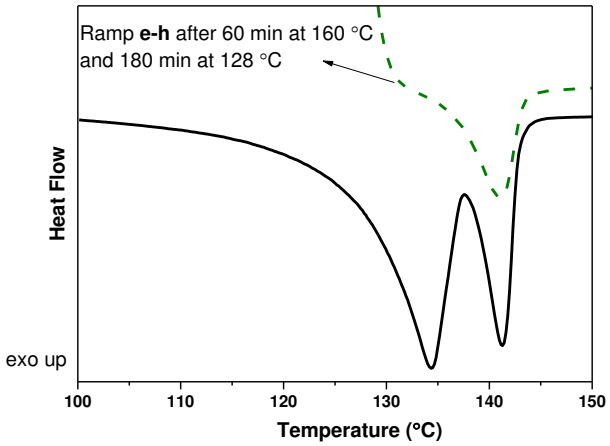

Figure 5 Dash green line is DSC plot obtained by new pathway e-h in Scheme 1. The disentangled UHMWPE sample is annealed at 160 ºC for 60 min and isothermally crystallized at 128 °C for 180 min. The endothermic peak results into an enthalpy of 26 J/g. For comparison, ramp g-h of Scheme 1 of a same disentangled sample, after the same heat treatment (160 ºC for 60 min and 128 ºC for 180 min), but with cooling, is also displayed in the figure. The enthalpy involved in the high temperature peak is approximately 34 J/g. The difference in enthalpy is attributed to crystallization on cooling. For details on the enthalpy values please refer to Table S5 in the supplementary section.

This further confirms that crystals responsible for high melting endothermic peak are formed at 128 ºC, whereas the crystals that give low temperature endothermic peak crystallize during dynamic cooling, e-f, in Scheme 1.

The influence of entanglements on nucleation density is in agreement with the earlier findings where Hikosaka and co-workers demonstrated that with the increasing entanglements, nucleation density decreases [12,13,14,15]. To recall, for their study the authors also created disentangled state but in a low molar mass high density polyethylene either by polymerization or by crystallizing the sample from melt in the hexagonal phase at high pressure and temperature. The sample in disentangled state showed higher nucleation density compared to its entangled state, which was achieved on annealing the same sample in melt.

3.1.1 Recurrence of high melting temperature peak independent of thermal history

On summing up the findings on the polymers synthesized using the single-site catalyst and the commercial sample, it can be conclusively stated that in disentangled UHMWPE

(regardless of molar mass) the decrease in the enthalpy of the high temperature peak with the annealing time arises from the entanglement formation. For the samples crystallized at 128 °C for the same isothermal crystallization time, the enthalpy of the high temperature endothermic peak decreases with annealing time at 160 °C, Figure 2. However, when the disentangled sample after reaching the equilibrium melt state (independent of its thermal history) was left at the isothermal crystallization temperature of 126 °C, Figure 6a, the high temperature endothermic peak at approximately 141.5 °C recurs and becomes prominent. Independent of the annealing times in melt state, the samples having different entanglement density, nearly no difference in enthalpy of the high temperature endothermic peak could be observed, Figure 6a. The recurrence of the high temperature melting peak on isothermal crystallization at 126 ^{o}C can be definitely explained by the lower nucleation barrier, compared to that at 128 ^{o}C, for crystallization. However, the absence of the same recurrence phenomenon in the comparative entangled sample (Figure 3b) leading to high melting temperature peak not higher than 135 ^{o}C in contrast to 141.5 ^{o}C (close to the equilibrium melting temperature for linear polyethylene) for the disentangled sample clearly indicates differences in the entangled state formed after polymerization and those created during polymerization. The latter is the case for the samples synthesized in the commercial conditions, using Z-N catalyst at high temperatures and pressures with the goal to have high catalyst activity. In contrast, the disentangled samples are synthesized in the controlled polymerization conditions at low temperatures using a single-site catalytic system, meeting the requirement of lesser number of entanglements (or connectivity) between the neighbouring crystals. On melting of the disentangled crystals, with the adoption of the random coil conformation, free volume between the chains is minimized by mixing process of the neighbouring chains followed by chain reptation. The chain reptation requires free chain ends that by weaving process will ultimately result into hooked entanglements. Considering the lesser number of chain ends in a polymer having high number average molar mass, compared to the low molar mass polyethylene, the weaving in of chains leading to hooked entanglements will be hindered. Moreover, the cooperative motion in the UHMWPE required for chain reptation for weaving in of the chains also get restricted. These possibilities do raise question on the differences in the nature of entangled state created after polymerization or entanglements established during polymerization. The differences in the topological constraints in melt of the UHMWPE samples arising due to polymerization conditions are realized during crystallization.

The DSC observations in Figure 6a do question the nature of chain interaction between the neighboring chains leading to differences in physical cross-links (entanglements), and their influence on topological variations in the non-crystalline region during crystallization. We would like to state further that independent of the annealing temperature, the associated annealing time, and the sample history, the recurrence of the high melting temperature peak is observed at the isothermal crystallization temperature of 126 ^{o}C (Figure 6b), which is triggered by the low nucleation barrier at this specific undercooling.

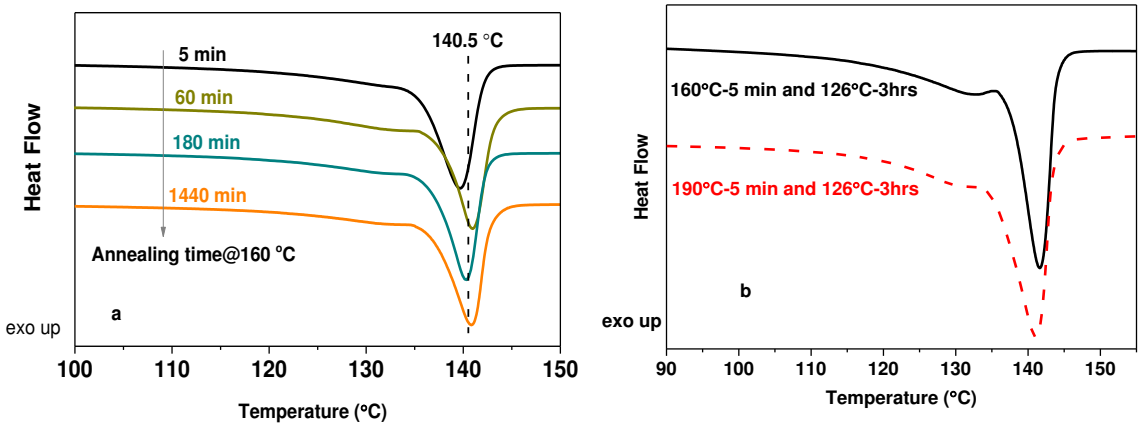

Figure 6 a) DSC plots, obtained from ramp g-h of Scheme 1, of the disentangled UHMWPE samples annealed at 160 ºC for different times and isothermally crystallized at 126 °C for 180 min **b)** Unlike the samples in 6a where the studies were performed solely in DSC pans, for figure 6b the samples investigated were taken after performing rheological studies. The modulus build-up of these samples was followed in Ares-rheometer. The samples investigated reached the equilibrium melt state, having storage modulus of 2 MPa, in the rheometer at 160 ºC after 24 hrs. DSC plots, obtained from ramp g-h of Scheme 1, of thus equilibrated disentangled UHMWPE samples were annealed at different temperatures in DSC (160 ºC and 190 ºC) for 5 min and isothermally crystallized at 126 ºC for 180 min; the continuous black line represents an equilibrated sample that was annealed at 160 ºC and the red dashed line represents an equilibrated sample that was annealed at 190 ºC.

In Figure 6b, the two equilibrated samples (where transformation from non-equilibrium to equilibrium melt state was followed in rheometer following the procedure applied for the Dis-PE-1 sample in Figure 1a) were annealed in DSC at different temperatures, 160 ºC and 190 ºC. The high temperature endothermic peak of both samples recurs and become prominent on isothermal crystallization at 126 ºC. Small difference can be observed in enthalpy of the high melting peaks. The recurrence of high melting peak, independent of thermal history, i.e. annealing temperature and time, may be attributed to differences in the entangled states perceived after polymerization via conventional route or entanglements created by mixing and chain reptation of initially disentangled polymers.

3.1.2 Equivalence in the rheological and thermal response of non-equilibrium polymer melt

In Figure 2, the low temperature endothermic peak, when normalized by the total enthalpy of the two endothermic peaks, shows increase with increasing annealing time in melt. The rate at which the low temperature endothermic peak increases shows strong dependence on the molar mass. For example, the time required for the increase in the enthalpy of the low temperature peak is longer for the higher molar mass. Such an example is depicted in Figure 7 where the observed trend is in agreement with the modulus build-up of the disentangled UHMWPE by rheology. The figure shows good correlation between the thermal and rheological response of the non-equilibrium polymer melts having different molar masses. The increase confirms the influence of entanglement formation on crystallization.

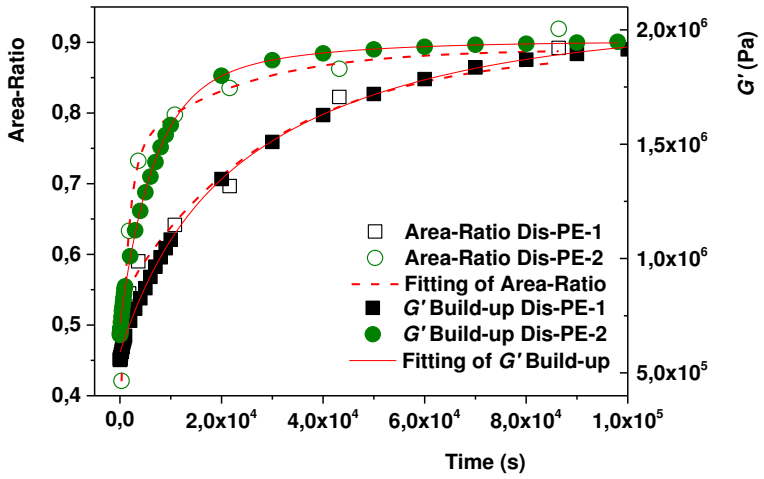

Figure 7 Area-ratio of the low temperature endothermic peak to the overall endothermic peaks, versus annealing time at 160 °C, of Dis-PE-1 (open squares) and Dis-PE-2 (open cycles), and storage modulus build-up of Dis-PE-1 (filled squares) and Dis-PE-2 (filled cycles); the rheological measurements are carried out at 160 °C, at a frequency of 10 rad/s and strain of 0.5 % (within the linear viscoelastic regime). Both the area-ratio and the build-up curves follow the trend depicted by equation (2).

In Figure 7, clear overlay between the area-ratio and *G'* build-up is observed, indicating that the crystallization kinetics is dominated by the change in entanglement density. This further confirms transformation of the heterogeneous melt from non-equilibrium to equilibrium melt state. Similar to the build-up in elastic shear modulus; the area-ratio shows an initial low value, followed by its increase with annealing time. Ultimately with time the area-ratio reaches a constant value where the high temperature endothermic peak almost vanishes. The low initial value, represents high enthalpy of the high temperature endothermic peak that

corresponds to a high amount of chains in a low entanglement state. The subsequent increase in the area-ratio is related to the increase in the enthalpy of the low temperature endothermic peak. The consequent decrease in the enthalpy of the high temperature endothermic peak is associated with the transformation of the heterogeneous distribution of entanglement density to homogeneous state. Using rheology the influence of the molar mass on the entanglement formation of disentangled UHMWPE has been investigated by Pandey et al. [21]. It has been shown that polymer with higher M_w takes longer time for the modulus to reach the thermodynamic equilibrium melt state. This is also seen in the crystallization behaviour of the polymer melts having chains with different molar masses. Retrospectively, difference in entanglement density between the two molar masses at the same annealing time, Figure 7, is evident from the storage modulus (circles and squares symbols).

Dis-PE-1, having the higher molar mass of 5.0 x 10^6 g/mol, takes longer time to reach its equilibrium state, so the non-equilibrium heterogeneous melt survives for longer time. As a result, the increase in the low melting peak area is delayed compared to that of Dis-PE-2 having low molar mass.

The modulus and area-ratio build-up can be divided into two regions: region I, a quick build-up at short times due to chain explosion and mixing; region II, a slow build-up for long time due to chain reptation and further entanglement. To have a quantitative estimation of the chain entanglement and relaxation in the two different regions, equation (2) is applied to fit both the rheology and the area-ratio, which was first proposed by Yamazaki et al. [14] followed by Teng et al. [28].

$$A(t) = A_N^0 - \sum_{i=1}^{N} \mathrm{A}_i \exp\left(\frac{-t}{\tau_i}\right) \quad (2)$$

A(t) is the modulus or the area-ratio at time t, A_N^0 is the plateau value of storage modulus build-up or the plateau value of the area-ratio, A_i is the increment in elasticity in modulus build-up or area-ratio in crystallization, corresponding to the relaxation mode with characteristic time τ_i. Two modes are used to fit the curves, in order to match the two-step build-up behaviour defined for disentangled UHMWPEs. The first mode at short times, τ_1, can be attributed to entropic mixing of the disentangled chains and the second mode at longer times of τ_2 is related to the further chain diffusion. Details of the fitting using two modes for disentangled UHMWPE are reported in ref [29]. The fitting curves are shown in Figure 7, where the fitting lines for the area-ratio are dotted and the fitting lines for the modulus build-

up are continuous. The fitting parameters for Dis-PE-1 and Dis-PE-2 in both cases of modulus build-up and area-ratio are shown in Table 2.

Table 2 Fitting parameters of the polymers (Dis-PE-1 and Dis-PE-2) investigated in this work: from modulus build-up and area-ratio respectively (A_1 and A_2 are normalized by their plateau values of area-ratio (crystallization) or elastic shear modulus build-up (rheology)).

Polymer	**A_1**	**A_2**	**τ_1 (s)**	**τ_2 (s)**
Dis-PE-1 (Rheology)	0.21	0.50	9579	40528
Dis-PE-1 (Crystallization)	0.11	0.39	853	29346
Dis-PE-2 (Rheology)	0.51	0.12	6461	25139
Dis-PE-2 (Crystallization)	0.44	0.17	1470	21206

Considering the two different experimental techniques and the involved methodology, reasonable agreement is observed in fitting parameters between the rheological and the thermal data of the two polymers, suggesting that change in the area-ratio of enthalpy is indicative of the entanglement formation in the same way as the elastic modulus build-up. It is apparent that the modulus build-up and area-ratio of Dis-PE-1, having higher molar mass, show lower A_1 compared to that of Dis-PE-2. The lower A_1 can be attributed to low initial entanglement density of the polymer. Pandey et al. also reported similar trend in their study on disentangled UHMWPEs [21]. Both fittings of the area-ratio and the modulus build-up show that reptation time τ_2 of Dis-PE-2 is lower than the values for Dis-PE-1. The low τ_2 for low molar mass indicates that time required for the low molar mass sample to reach the equilibrium state is less than the high molar mass sample. Independent of the methods used, rheology or thermal, the time required for entropic mixing (τ_1) compared to reptation time (τ_2) is relatively small. To recall, the observations by NMR are that the time needed for entropic mixing scales with $M_n^{0.7}$, whereas the overall modulus build-up scales with approximately $M_n^{3.0}$. For details please refer to Figure 2.12 of reference [30] and reference [21].

The combination of the above findings on disentangled UHMWPE, together with the studies performed on the entangled commercial sample, rules out the possible memory effect [31] as an explanation for the increase in the low melting temperature enthalpy at an expense of the high melting temperature peak with annealing time in melt. The influence of the melt memory effect on the presence of the high temperature melting peak is further ruled out by the experiments reported in section 0.1, Figure 6. The recurrence of the high melting

temperature peak (141.5 °C) at 126 °C independent of the annealing temperature and annealing time in melt, Figure 6, reflects the differences in the entangled nature achieved in the sample synthesized using the single-site catalytic system, compared to the Z-N catalyst. A similar high temperature endothermic peak, under similar crystallization conditions, is observed in the polymer synthesized using the Z-N catalyst, but at much lower temperature (134.5 °C). Thus it is important to realise that the inversion in enthalpy during the transformation of non-equilibrium melt into equilibrium state is an intrinsic property of the polymer synthesized using the single-site catalytic system, Figure 2.

3.2 Annealing temperature in Scheme 1 and its influence on the crystallization kinetics

The influence of annealing temperature in melt state on the entanglement formation and its influence on crystallization are depicted in Figure 8. The samples of Dis-PE-2 are annealed at different temperatures: 160 °C, 170 °C, 180 °C and 190 °C for 60 min followed by isothermal crystallization at 128 °C for 180 min. From Figure 8 it is evident that with increasing melt temperature (annealing temperature), the high temperature endothermic peak, related to the crystals formed from disentangled domains decreases. This indicates increase in the rate of entanglement formation with increasing annealing temperature. The increase is attributed to the higher chain mobility at higher annealing temperature. The increase is in accordance with the rheological studies on the disentangled UHMWPE, where the time required for the elastic shear modulus to reach the equilibrium melt state is reported to be shorter at higher annealing temperatures [11]. As shown in Figure 6b, independent of the annealing temperature the recurrence in the high melting temperature peak could be observed. These findings further strengthen the influence of polymerization conditions on the resultant melt state, where the possibility of different topological constraints built in during polymerization or created after polymerization in these high molar masses seem to differ. The differences in the topological constraints result into crystals having significantly different melting points. The differences in the topological constraints in the melt state of the polymers, synthesized using the two different polymerization conditions (used in the present case for the single-site and Z-N), are likely to influence the topology of non-crystalline domains in the semi-crystalline polymer. The difference in melt topology ultimately leads to the possibility of the recurrence of high melting temperature. Here we recall our earlier studies on the influence of chain topology on melting kinetics [10,11]. We have shown that the high melting temperature of the chain folded nascent crystals of UHMWPE is the result of constrained non-crystalline region [32].

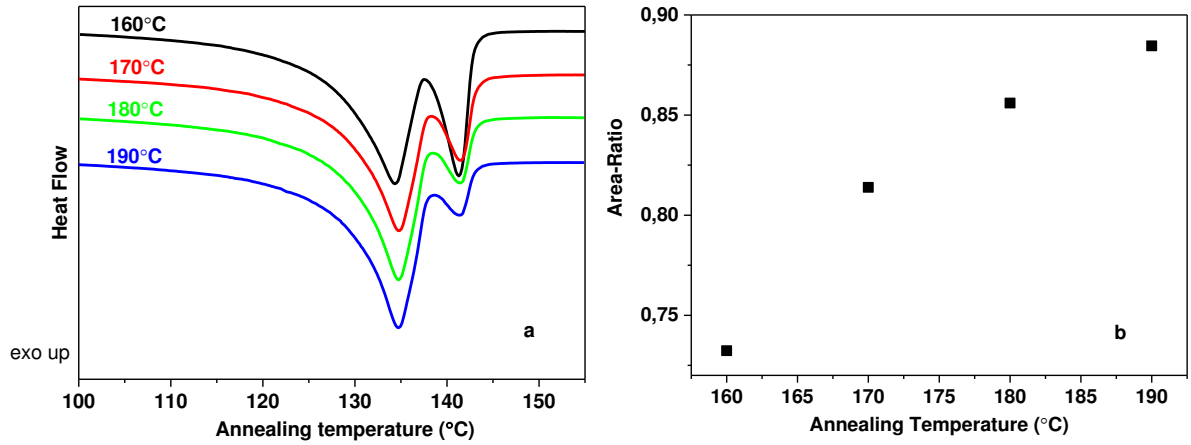

Figure 8 a) DSC heating runs, plotted from ramp g-h of Scheme 1, of Dis-PE-2, after annealing at 160, 170, 180 and 190 °C for 60 min, respectively and followed by 180 min isothermal crystallization at 128 °C; b) area-ratio of the enthalpy of low temperature endothermic peak to the overall endothermic peak, as a function of annealing temperature.

3.3 Retention of non-equilibrium melt state in the presence of graphene

The correlation between the rheological and the thermal response of disentangled polymer melt is further strengthened by exploring the chain filler interaction. To recall, it is shown in Figure 9d, and Figure 7b of ref [17] that in the presence of a specific concentration of rGON (0.8 wt %), the elastic shear modulus build-up is restricted to an extent that within the experimental time scale, at 160 °C, negligible increase in the modulus is observed reflecting the survival of a long-lasting non-equilibrium melt. In this section we aim to investigate the thermal response of the long-lasting non-equilibrium melt on crystallization in the presence of rGON. The experimental protocols are the same as that for the same polymer without the filler, Figure 2a and Figure 3.

The nascent UHMWPE powder mixed with rGON, after drying, is directly used for the thermal analysis. The mixing is performed using the method described in ref [17]. The heating runs after annealing at 160 °C for different times followed by 180 min isothermal crystallization at 128 °C are summarized in Figure 9, where Figure 9a and Figure 9b show the results of 0.1 wt % and 0.8 wt % composites, respectively. The normalized low temperature endothermic peak, for both composites and the pure polymer are shown in Figure 9c, whereas Figure 9d shows the corresponding rheological response of the samples.

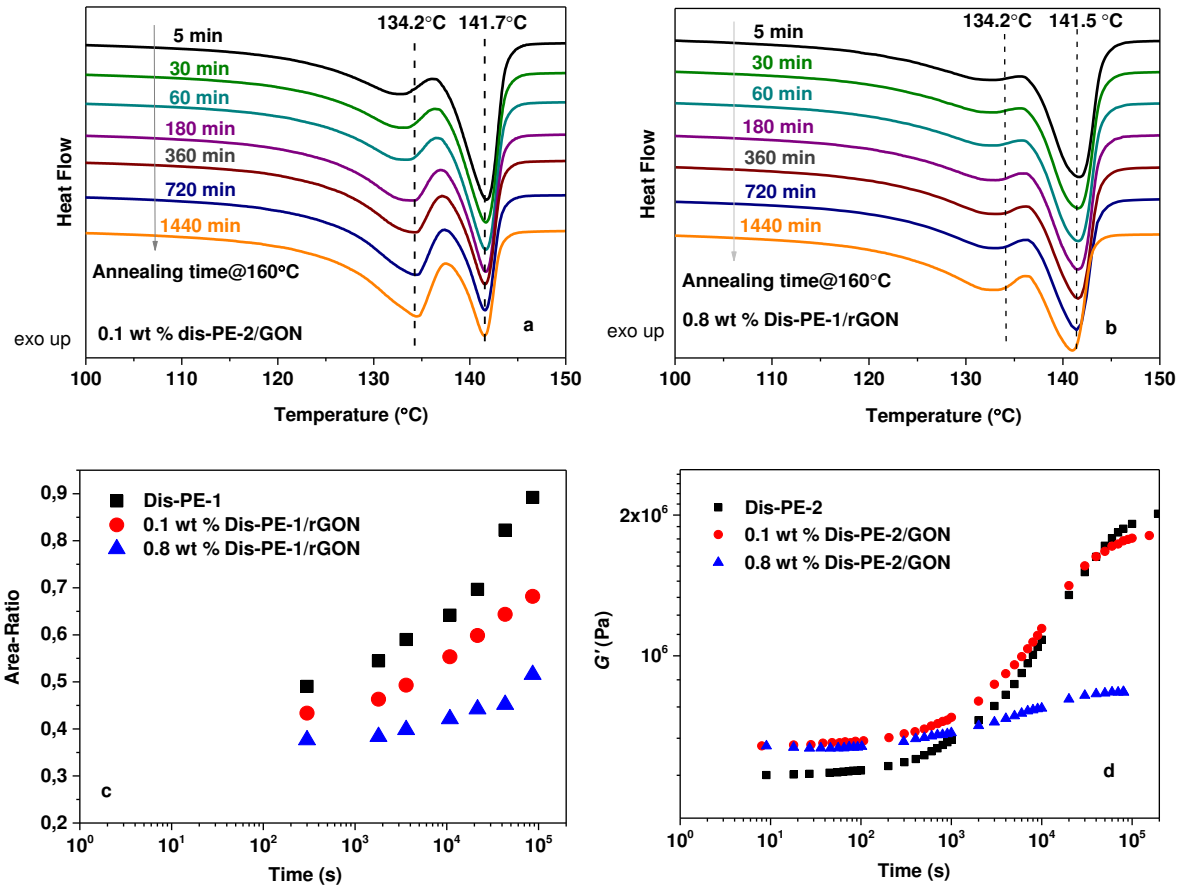

Figure 9 DSC heating runs after different annealing times at 160 °C followed by 180 min isothermal crystallization at 128 °C of **a)** 0.1 wt % Dis-PE-1/rGON and **b)** 0.8 wt % Dis-PE-1/rGON composites; **c)** normalized low temperature endothermic peak as a function of annealing time at 160 °C, of Dis-PE-1, 0.1 wt % Dis-PE-1/rGON and 0.8 wt % Dis-PE-1/rGON, and **d)** elastic shear modulus build-up of Dis-PE-1, 0.1 wt % Dis-PE-1/rGON and 0.8 wt % Dis-PE-1/rGON samples.

From Figure 9a and 9b, it is apparent that the decrease in the enthalpy of the high temperature endothermic peak with increasing annealing time in melt is suppressed in the presence of rGON. The suppression becomes more pronounced when the filler concentration increases. At rGON concentration of 0.8 wt %, both low and high temperature endothermic peak areas are found to be nearly independent of the annealing time at 160 °C, suggesting that the heterogeneous melt state, having heterogeneity in the distribution of entanglements, survives for at least the given experimental time. In Figure 9c and 9d, the changes in the enthalpy area-ratio are found to follow trend similar to the elastic shear modulus build-up, starting from low values. The modulus build-up is the slowest for the sample having 0.8 wt % of the filler concentration. In both thermal and rheological studies, the retardation in enthalpy and shear elastic modulus build-up is attributed to the strong chain-filler interaction that arrests the dynamic of the disentangled chains, keeping them less entangled for longer times. The

presence of low entangled regions, at a filler concentration of 0.8 wt %, enhances the nucleation rate and thus facilitates the overall crystallization rate during isothermal crystallization at 128 ºC, giving rise to little change in the high temperature endothermic peak. It is important to mention that the presence of rGON could also enhance the nucleation rate of the less entangled chains by enhancing the nucleation efficiency and further accelerating the crystallization rate of chains during isothermal crystallization [33].

To have insight into the influence of the filler on the double peaks in the disentangled UHMWPE, the protocol for Figure 3 is also applied to the composite sample having 0.8 wt % rGON, and the results are shown in Figure 10. Similar to the nascent sample without the filler in Figure 3a, in the composite the observations are that the endothermic peak on heating from g-h shows a gradual shift from 135 °C to 141.5 °C with increasing crystallization temperature from 120 °C to 126 °C. At 128 °C, a low temperature endothermic peak, on heating the sample along g-h, starts to appear though the enthalpic contribution is relatively less than in the sample without the filler (see Figure 3).

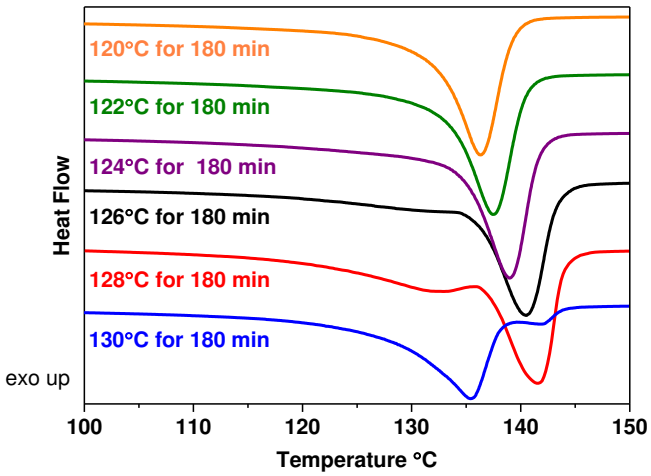

Figure 10 DSC plots, obtained from ramp g-h of Scheme 1, of 0.8 wt % Dis-PE-1/rGON sample annealed at 160 ºC for a fixed time and isothermally crystallized for 180 min at different temperatures.

To strengthen the response of the enthalpic relaxation specific to the disentangled polymer synthesized using the single-site catalytic system, a comparative study of a commercial sample in the presence of rGON (C-PE/rGON) is also performed. The thermal protocol in Figure 11 for the 0.8 wt % C-PE/rGON composites is similar to that applied for the 0.8 wt % Dis-PE-1/rGON composites (Figure 9b). Unlike in the case of the 0.8 wt % Dis-PE-1/rGON composites no high temperature endothermic peak is observed in the commercial composite sample. The observations are similar to C-PE samples without rGON, Figure 2b. Thus the

influence of rGON on the observed changes in the disentangled sample Figure 9b, synthesized using the single-site catalytic system, are attributed to the intrinsic nature of the heterogeneous melt state.

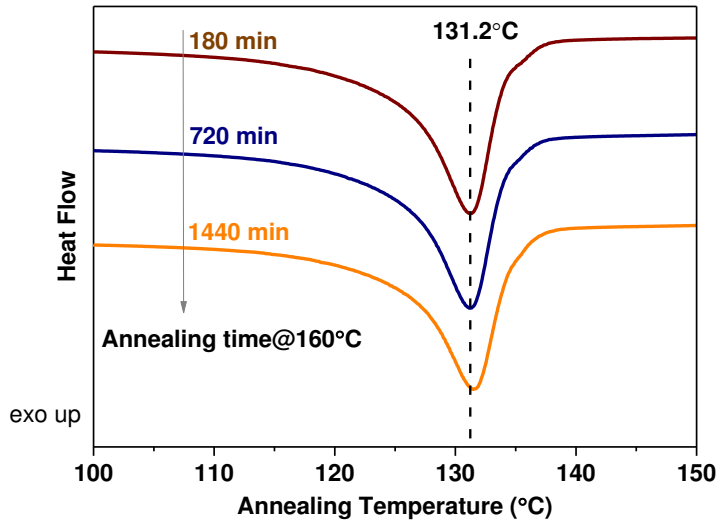

Figure 11 DSC heating runs of C-PE/0.8 wt % rGON sample after different annealing times (180 min, 720 min and 1440 min) followed by 180 min isothermal crystallization at 128 °C.

Figure 12 summarizes the total melting enthalpies of the samples with increasing annealing time. A significant decrease in the enthalpy of dis-PE sample is observed, compared to that of entangled UHMWPE samples, and it can be attributed to the entanglement process. However, in the presence of rGON, the suppression in entanglement formation causes the presence of disentangled domains that favours nucleation and no change in the overall enthalpy is observed, Figure 12. Furthermore, these results also rule out the possibility of any thermal oxidation of the samples in the presence of rGON.

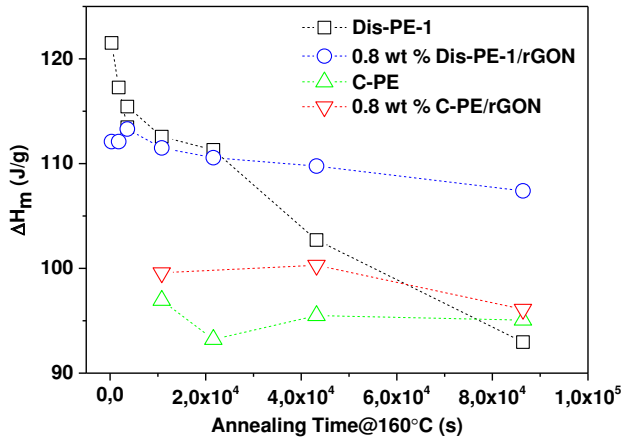

Figure 12 Total melting enthalpies versus increasing annealing time at 160 ºC of both disentangled and commercial entangled UHMWPE samples with and without rGON. The enthalpies are calculated from Figure 2a, Figure 2b, Figure 9b and Figure 11, which are obtained from ramp g-h of Scheme 1. The lines are drawn for the guidance.

In a recent publication by Weir et al. [34] making use of neutron scattering, the authors have also conclusively demonstrated reduction in the entanglement network of PMMA in the presence of graphene oxide. The reduction of the entanglement density has been supported by rheological studies demonstrating minima in the storage modulus at a specific concentration of graphene oxide. These findings by Weir et al are in agreement with our earlier reported observations on UHMWPE and rGON [17]. In addition, the authors have investigated distortion in chain conformation in the presence of graphene oxide.

3.4 Interaction between rGON and the disentangled UHMWPE

To have further insight between the interaction of rGON with disentangled UHMWPE chains, NMR studies have been performed. Figure 13a shows one-dimensional (1D) ^{1}H NMR spectrum of disentangled UHMW-PE (at chemical shift 0-3 ppm) and the filler (5-7 ppm). The assignment of the interaction between PE and the filler was made tentatively on the Dis-PE-1/rGON sample having good dispersion of the filler. The 2D exchange spectrum with exchange time τ = 40ms exhibits strong cross peaks that connect protons from functional groups of the filler with protons of the polyethylene. These cross-peaks arise from the exchange of nuclear magnetization via intramolecular spin diffusion during exchange process, τ, indicating the presence of strong physical interactions between the filler and the matrix.

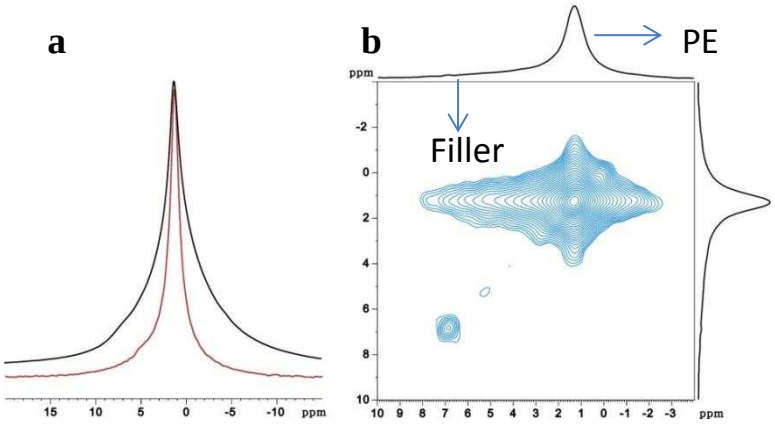

Figure 13 a) 1D spectrum (out line is the sp, inner line is Hahn Echo L1=1), and **b)** Carbonyl region of the 2D exchange spectrum ^{1}H NMR (Hahn-Echo-NOSEY L1=1 d6=40ms) of 0.8 wt % Dis-PE-1/rGON (right).

The interaction of ethylene segments with carbon based filler has also been conclusively demonstrated by Litvinov and co-workers in the studies on ethylene propylene diene rubber (EPDM)/carbon black composites by NMR, where the authors showed the interaction is due to the adsorption of ethylene segments to the large surface of carbon filler [35,36]. Moreover, it is reported that among all carbon based nano-fillers, graphene has the strongest interaction with PE matrix, as shown by the molecular dynamic simulations of PE nanocomposites with different carbon based fillers [37,38]. In summary, the strong chain-filler interaction supported by NMR studies strengthens our findings on thermal and rheological response of the composites.

4.0 Graphic Illustration of the Experimental Findings

In this section experimental findings on the recurrence of high melting temperature have been illustrated graphically. Due to high catalyst activity and high polymerization temperature, during the conventional Z-N polymerization conditions, the entanglements are established at the very birth of the polymer (Figure 14). On the other hand, when a single-site catalytic system in combination with low polymerization temperature is used for synthesis, entanglement density in the non-crystalline region is considerably reduced. The difference in the entanglement density in the semi-crystalline polymer, established during polymerization, results into ease in solid-state uniaxial deformation of the polymer [22,1].

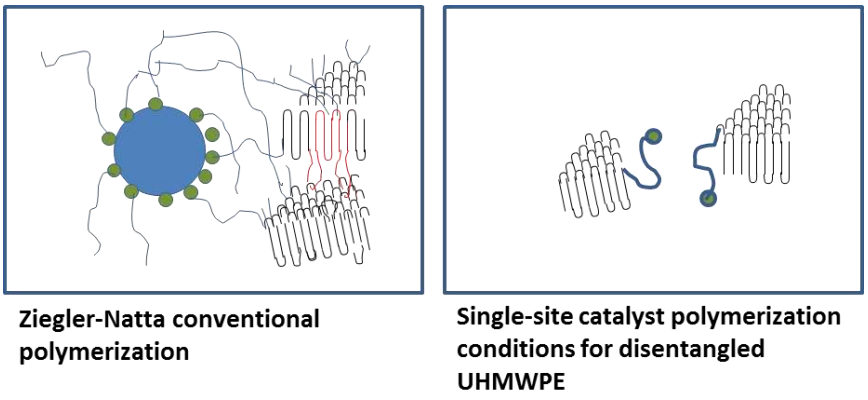

Figure 14 Differences in active site density and its influence on entanglement formation is illustrated. Substrates having anchored active catalyst sites with differences in their density are depicted in the figure. When chain growth is higher than the crystallization rate, entanglements are formed prior to crystallization.

Figure 15 provides illustration on melting and crystallization of the samples synthesized using the two different catalytic systems. On melting, the heterogeneous distribution of entanglements confined in the non-crystalline region of the semi-crystalline polymer tends to homogenize. The homogenization process of entanglements in the conventional commercial sample occurs much faster compared to the disentangled UHMWPE having considerably low number of entanglements between the crystals. As stated earlier, the homogenization process of entanglements in the disentangled polymer follows the power law $t_{build\text{-}up} \sim M_n^{3.0}$ [21].

Considering the high M_n of the disentangled UHMWPE, the possibility of entanglement formation via chain reptation, ultimately leading to conventional hooked entangled state between chains is questioned. Most likely the conformational restriction, leading to the virtual tube formation along the test chain, is established by physical contact between the neighbouring chains – the unhooked entanglements. During crystallization under the isothermal condition (126 ^{o}C) (in section 1.3.1.1), the unhooked entanglements do not provide same restriction as the hooked entanglements for disengagement of chains. Thus influencing the topology of the non-crystalline region and retrospectively increasing the melting temperature [32].

To recall, these results are further supported by elastic shear modulus build-up of disentangled UHMWPE/rGON composites at different temperatures (160 ºC and 190 ºC). Recently, it has been reported that the presence of graphene as a filler reduces entanglement network [17,18,34] in melt, (Figure 9d), having implications on the recurrence of high melting temperature peak in DSC (Figure 9b).

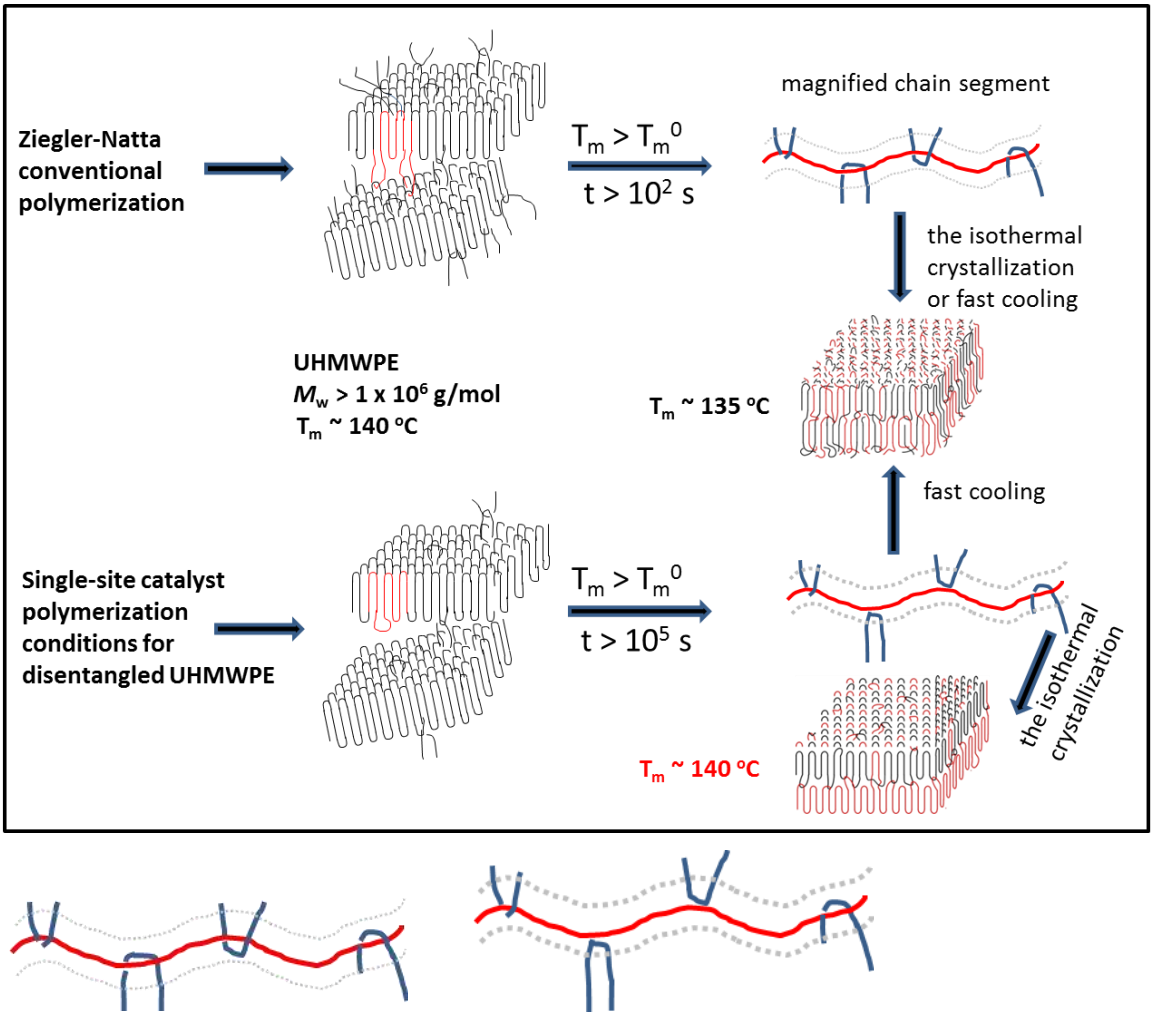

Figure 15 The figure illustrates the differences in the entangled states of the non-crystalline regions of the semi-crystalline UHMWPE at different stages of experiments conducted in this study. The magnified chain segment with differences in topological constraints, unhooked (crossing over of chains) and hooked (contact between the chains) is depicted in the illustration below. Independent of the nature of the topological constraints between chain segments, the presence of de Gennes virtual tube is likely to be realized. However, required cooperative motion to create hooked entanglements in these ultrahigh molecular weight polymer melt, having low number of chain ends, can be questioned.

5.0 Conclusions

We have investigated the crystallization kinetics and associated melt enthalpies of isothermally crystallized disentangled UHMWPE samples from non-equilibrium melt having different entanglement densities. The two peaks, observed after annealing the polymer at 160 °C and isothermal crystallization, are attributed to the heterogeneous distribution of entanglement density having different response to crystallization. The less entangled domains, having higher nucleation rates, form crystals that on melting correspond to high temperature endothermic peak, whereas the entangled domains having higher nucleation barrier requires

higher supercooling for crystallization. The entangled domains crystallize on cooling below the chosen isothermal crystallization temperature. It is also found that the low temperature endothermic peak increases at the expense of the high temperature endothermic peak with annealing time at 160 °C, following the trend similar to the increase in elastic shear modulus with entanglement formation. The molar mass also shows an influence on the entanglement formation and consequently on crystallization. The entanglement formations in the non-equilibrium melt progresses faster with increasing the annealing temperature. We also demonstrate that in the presence of rGON, the high temperature endothermic peak, i.e. the less entangled domains, is less influenced by annealing time in the melt, and at the filler concentration of 0.8 wt %, the peak is almost independent of the annealing time. We have attributed this phenomenon to strong chain-filler interaction that arrests chain dynamics and thus supresses the chain entanglement formation. The chain-filler interaction is further investigated and supported by solid-state NMR.

The thermal analysis on disentangled UHMWPE also addresses the recurrence of high melting temperature peak (141.5 ^{o}C) in the samples where entanglements are created after polymerization. The differences in the topological constraints build up during and created after polymerization seems to have strong influence on the recurrence of the high melting temperature peak. These findings do question the nature of the entanglement formation in the initially non-equilibrium melt state. For comparison, studies have been performed on commercial sample synthesized using a Z-N catalyst.

References

[1] Rastogi, S.; Yao, Y.; Ronca, S.; Bos, J. and van der Eeem, J. Unprecedented high-modulus high-strength tapes and films of ultrahigh molecular weight polyethylene via solvent-free route, Macromolecules **2011**, 44, 5558-5568

[2] Wittmann, J. C.; Lotz, B. J. Polymer decoration; The orientation of polymer folds as revealed by the crystallization of polymer vapors.; J. Polym. Sci., B Polym. Phys. Ed. **1985**, 23(1), 205-226.

[3] Yin, L.; Chen, J.; Yang, X.; Zhou, E. Structure image of single crystal of polyethylene. Polymer **2003**, 44, 6489-6493.

[4] Talebi, S.; Duchateau, R.; Rastogi, S.; Kaschta, J.; Peters, G. W. M.; Lemstra, P. J. Molar mass and molecular weight distribution determination of UHMWPE synthesized using a living homogeneous catalyst. Macromolecules **2010**, 43 (6), 2780-2788.

[5] Rastogi, S.; Lippits, D. R.; Peters, G. W. M.; Graf, R.; Yao, Y.; Spiess, H. W. Heterogeneous in polymer melts from melting of polymer crystals. Nat. Mater. **2005**, 4, 635-641.

[6] Tapash, A.; DesLauriers, P. J.; White, J. L. Simple NMR experiements reveal the influence of chain and chain architecture on the crystalline/amorphous interface in polyethylene. Macromolecules **2015**, 48(9), 3040-3048.

[7] Yao, Y.; Rastogi, S.; Xue, H.; Chen, Q.; Graf, R.; Verhoef, R. Segmental mobility in the non-crystalline regions of nascent polyethylene synthesized using two different catalytic systems with implications on solid state deformation. Polymer **2013**, 54 (1), 411-422.

[8] Keller, A. A note on single crystals in polymers: evidence for a folded chain configuration. Philos. Mag. Ser. **1957**, 8(2), 1171-1175.

[9] Sadler, D. M. New explanation for chain folding in polymers. Nature **1987**, 326, 174-177.

[10] Lippits, D. R.; Rastogi, S.; Höhne, G. W. H. Melting kinetics in polymers. Phys. Rev. Lett. **2006,** 96, 2006, 218303

[11] Pandey, A.; Toda, A.; Rastogi, S. Influence of amorphous component on melting of semicrystalline polymers. Macromolecules **2011**, 44, 8042-8055 and Pandey, A. V. Nonlinear viscoelastic response of a thermodynamically metastable polymer melt. PhD Thesis **2011**. Loughborough University.

[12] Yamazaki, S.; Hikosaka, M.; Gu, F.; Ghosh, S. K.; Arakaki, M.; Toda, A. Effect of entanglement on nucleation rate of polyethylene. Polymer J. **2001**, 33 (11), 906-908.

[13] Yamazaki, S.; Hikosaka, M.; Toda, A.; Wataoka, I.; Gu, F. Role of entanglement in nucleation and 'melt relaxation' of polyethylene. Polymer **2002**, 43, 6585-6593.

[14] Yamazaki, S.; Gu, F.; Watanabe, K.; Okada, K.; Toda, A.; Hikosaka, M. Two-step formation of entanglement from disentangled polymer melt detected by using nucleation rate. Polymer **2006**, 47, 6422-6428.

[15] Hikosaka, M.; Watanabe, K.; Okada, K.; Yamazaki, S. Topological mechanism of polymer nucleation and growth-the role of chain sliding diffusion and entanglement. Adv. Polym. Sci. **2005**, 191, 137-186.

[16] Liu, P.; Gong, K.; Xiao, P.; Xiao, M. Preparation and characterization of poly(vinyl acetate)-intercalated graphite oxide nanocomposite. J. Mater. Chem. **2000**, 10, 933-935.

[17] Liu, K.; Ronca, S.; Andablo-Reyes, E.; Forte, G.; Rastogi, S. Unique rheological response of Ultrahigh Molecular Weight Polyethylenes in the presence of reduced graphene oxide. Macromolecules **2015**, 48(1), 131-139.

[18] Liu, K.; Andablo-Reyes, E.; Patil, N.; Merino, D. H.; Ronca, S.; Rastogi, S. Influence of reduced graphene oxide on the rheological response and chain orientation on shear deformation of high density polyethylene. Polymer **2016**, 87, 8-16.

[19] Mead, D. Determination of molecular weight distributions of linear flexible polymers from linear viscoelastic material functions. J. Rheol. **1994**, 38, 1797-1827.

[20] Tuminello, W. H. Molecular weight and molecular weight distribution from dynamic measurements of polymer melts. Polym. Eng. Sci. **1986**, 26, 1339-1347.

[21] Pandey, A.; Champouret, Y.; Rastogi, S. Heterogeneity in the distribution of entanglement density during polymerization in disentangled ultrahigh molecular weight polyethylene. Macromolecules **2011**, 44(12), 4952-4960.

[22] Romano, D.; Tops, N.; Andablo-Reyes, E.; Ronca, S.; Rastogi, S. Influence of polymerization conditions on melting kinetics of low UHMWPE and its implications on mechanical properties. Macromolecules **2014**, 47(14), 4750-4760.

[23] Saito, J.; Mitani, M.; Matsui, S.; Sugi, M.; Tohi, Y.; Tsutsui, T.; Fujita, T.; Nitabaru, M.; Makio, H. Olefin polymerization catalysts, transition metal compounds, processes for olefin polymerization, and Alpha-olefin/conjugated diene copolymers. European Patent 0874005, 1997.

[24] Ferry, J. D. Viscoelastic Properties of Polymers, 3rd ed. Wiley: New York, 1980.

[25] Kovacs, A. J.; Gonthier, A.; Straupe, C. Isothermal growth, thickening, and melting of poly(ethylene oxide) single crystals in the bulk. J. Polym. Sci.: Symp. **1975**, 50, 283-325.

[26] Weeks, J. J. Melting temperature and change in lamellar thickness with time for build polyethylene. Journal of research of the national bureau of standards-A. Phys. Chem. **1963**, 67A(5), 441-451.

[27] Gopalan, M.; Mandelkern, L. The effect of crystallization temperature and molecular weight on the melting temperature of linear polyethylene. J. Phys. Chem. **1967**, 71(12), 3833-3841.

[28] Teng, C.; Gao, Y.; Wang, X.; Jiang, W.; Zhang, C.; Wang, R.; Zhou, D.; Xue, G. Reentanglement kinetics of freeze-dried polymers above the glass transition temperature. Macromolecules **2012**, 45, 6648-6651.

[29] Andablo-Reyes, E.; de Boer, E.; Romano, D.; Rastogi, S. Stress relaxation in the nonequilibrium state of a polymer melt. J. Rheol. **2014**, 58(6), 1981-1991.

[30] Lippits, D. R. Heterogeneity in polymer melts by controlled melting of polymer crystals PhD Thesis, **2007**, ISBN 978-90-386-0895-2 Eindhoven University of Technology.

[31] Alfonso, G.C.; Scardigli, P., Melt memory effects in polymer crystallization; Macromol. Symp. **1997,** 118, 323-328.

[32] Rastogi, S.; Lippits, D. R.; Hohne, G. W. H.; Mezari, B.; Magusin, P. C. M. M. The role of the amorphous phase in melting of linear UHMW-PE; implications for chain dynamics. J. Phys.: Condens. Matter. **2007**, 19 (20), 205122, 1-21.

[33] Xu, J. Z.; Zhong, G. J.; Hsiao, B. S.; Fu, Q.; Li, Z. M. Low-dimensional carbonaceous nanofiller induced polymer crystallization. Prog. Polym. Sci. **2014**, 39, 555-593.

[34] Weir, M. P.; Johnson, D. W.; Boothroyd, S. C.; Savage, R. C.; Thompson, R. L.; King, S. M.; Rogers, S. E.; Coleman, K. S.; Clarke, N. Distortion of Chain Conformation and Reduced Entanglement in Polymer−Graphene Oxide Nanocomposites. ACS Macro Lett. **2016**, 5, 430−434.

[35] Litvinov, V. M.; Steeman, P. A. M. Vulcanized siloxane chains swollen by polymer chains: NMR investigations into free-chain dynamics. Macromolecules **1999**, 32, 8476-8490.

[36] Litvinov, V. M.; Orza, R. A.; Klüppel, M.; Van Duin, M.; Magusin, P. C. M. M. Rubber-filler interaction and network structure in relation to stress-strain behavior of vulcanized, carbon black filled EPDM. Macromolecules **2011**, 44, 4887-4900.

[37] Cheng, S.; Chen, X.; Hsuan, G. Y.; Li, C. Y. Reduced graphene oxide-induced polyethylene crystallization in solution and nanocomposites. Macromolecules **2011**, 45, 993-1000.

[38] Li, Y. Effect of nano inclusions on the structural and physical properties of polyethylene matrix. Polymer **2011**, 52(10), 2310-2318.

TOC:

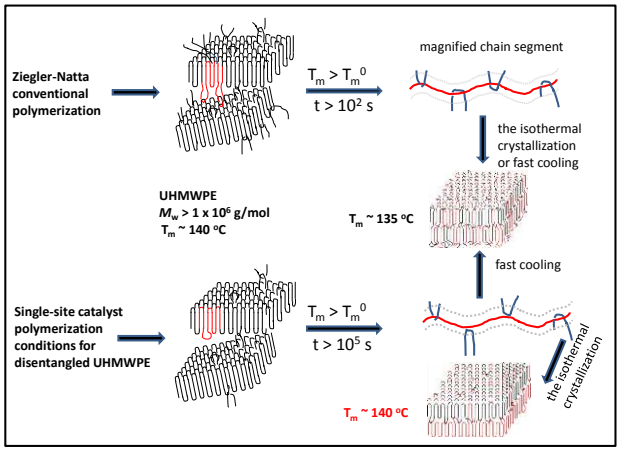
Ziegler-Natta conventional polymerization
UHMWPE
M_w > 1 x 10^6 g/mol
T_m ~ 140 °C
$T_m > T_m^0$
t > 10^2 s
magnified chain segment
the isothermal crystallization or fast cooling
T_m ~ 135 °C
fast cooling
Single-site catalyst polymerization conditions for disentangled UHMWPE
$T_m > T_m^0$
t > 10^5 s
T_m ~ 140 °C
the isothermal crystallization